Acta Pharmaceutica Sinica B 2016;6(3):212–221

Chinese Pharmaceutical Association
Institute of Materia Medica, Chinese Academy of Medical Sciences

Acta Pharmaceutica Sinica B

www.elsevier.com/locate/apsb
www.sciencedirect.com

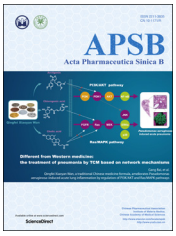

ORIGINAL ARTICLE

Qingfei Xiaoyan Wan, a traditional Chinese medicine formula, ameliorates *Pseudomonas aeruginosa*–induced acute lung inflammation by regulation of PI3K/AKT and Ras/MAPK pathways

Yuanyuan Hou[a,b], Yan Nie[a,b], Binfeng Cheng[a,b], Jin Tao[a,b], Xiaoyao Ma[a,b], Min Jiang[a,b], Jie Gao[a,b], Gang Bai[a,b,*]

[a]*State Key Laboratory of Medicinal Chemical Biology and College of Pharmacy, Nankai University, Tianjin 300071, China*
[b]*Tianjin Key Laboratory of Molecular Drug Research, Nankai University, Tianjin 300071, China*

Received 25 November 2015; received in revised form 4 February 2016; accepted 22 February 2016

KEY WORDS

Anti-inflammatory;
Network pharmacology;
Pathogenic bacterial infection;
PI3K/AKT pathway;
Ras/MAPK pathway;
Lung;
Mouse

Abstract Gram-negative pathogen–induced nosocomial infections and resistance are a most serious menace to global public health. Qingfei Xiaoyan Wan (QF), a traditional Chinese medicine (TCM) formula, has been used clinically in China for the treatment of upper respiratory tract infections, acute or chronic bronchitis and pulmonary infection. In this study, the effects of QF on *Pseudomonas aeruginosa*–induced acute pneumonia in mice were evaluated. The mechanisms by which four typical anti-inflammatory ingredients from QF, arctigenin (ATG), cholic acid (CLA), chlorogenic acid (CGA) and sinapic acid (SPA), regulate anti-inflammatory signaling pathways and related targets were investigated using molecular biology and molecular docking techniques. The results showed that pretreatment with QF significantly inhibits the release of cytokines (TNF-α and IL-6) and chemokines (IL-8 and RANTES), reduces leukocytes recruitment into inflamed tissues and ameliorates pulmonary edema and necrosis. In

Abbreviations: ATG, arctigenin; CGA, chlorogenic acid; CLA, cholic acid; Dex, dexamethasone; DMSO, dimethylsulfoxide; ELISA, enzyme-linked immunosorbent assay; ESI, electrospray ionization; GA, genetic algorithm; HE, hematoxylin and eosin; KEGG, Kyoto Encyclopedia of Genes and Genomes; LB, Luria–Bertani; LEV, levofloxacin; MAPK, mitogen activated protein kinase; NFATc1, nuclear factor of activated T cells c1; Ninj1, ninjurin1; PBS, phosphate-buffered saline; PI3K, phosphoinositide 3-kinase; QF, Qingfei Xiaoyan Wan; SARS, severe acute respiratory syndrome; SPA, sinapic acid; TCM, traditional Chinese medicine; TTBS, Tween 20/Tris-buffered saline; UPLC, ultra-performance liquid chromatography

*Corresponding author.
E-mail address: gangbai@nankai.edu.cn (Gang Bai).

Peer review under responsibility of Institute of Materia Medica, Chinese Academy of Medical Sciences and Chinese Pharmaceutical Association.

http://dx.doi.org/10.1016/j.apsb.2016.03.002

addition, ATG was identified as the primary anti-inflammatory agent with action on the PI3K/AKT and Ras/MAPK pathways. CLA and CGA enhanced the actions of ATG and exhibited synergistic NF-κB inactivation effects possibly *via* the Ras/MAPK signaling pathway. Moreover, CLA is speculated to target FGFR and MEK firstly. Overall, QF regulated the PI3K/AKT and Ras/MAPK pathways to inhibit pathogenic bacterial infections effectively.

1. Introduction

It may be a challenge to clarify traditional Chinese medicine (TCM) therapies because their mechanisms are usually unclear and many ingredients in these herbal formula may exert their effects by regulating multiple pathways and targets[1]. Recently, TCM has been considered to highlight targets in interconnected pathways that can be used to cure complex disease. The integration of TCM and "network" pharmacology provides an innovative approach for TCM theory of both reductionist and holistic medicine, and bridges traditional application and modern drug discovery[2,3]. TCM was widely used for the clinical treatment of infectious diseases for thousands of years in China, and it is based on different philosophies than those of Western medicine, which are based on antibiotics[4]. Now, TCM has also played an important role in the prevention and treatment of infection during several large respiratory disease outbreaks, such as severe acute respiratory syndrome (SARS) and acquired pneumonia[5,6]. Although the precise mechanisms of action remain unclear from the perspective of modern medicine, a therapeutic regimen combining Chinese and Western medicines has gained acceptance because it reduces resistance and toxicity.

Qingfei Xiaoyan Wan (QF) is a pill derived from a classic TCM prescription (Maxing Shigan decoction) and consists of eight common Chinese herbal medicines, Herba Ephedra, Gypsum Fibrosum, Pheretima, Fructus Arctii, Semen Lepidii, Bovis Calculus, Semen Armeniacae Amarum and Cornu Saigae Tataricae. QF is approved by the China Food and Drug Administration (No. Z12020757) and has been used clinically for the treatment of upper respiratory tract infection, acute bronchitis, acute exacerbation of chronic bronchitis and pulmonary infection with excellent clinical effects. In our previous studies, QF alleviates asthma and has anti-inflammatory activities[7,8]. Four types of NF-κB inhibitors, including arctigenin (ATG) derivatives, cholic acid (CLA) derivatives, chlorogenic acid (CGA), and sinapic acid (SPA), were screened[9] In this study, these anti-inflammatory compounds were quantified using an ultra-performance liquid chromatography (UPLC) system. The effects of QF on *Pseudomona aeruginosa*–induced lung infection in mice were investigated, and possible synergetic anti-inflammatory mechanisms for suppressing bacterial pneumonia by mutual regulation of the PI3K/AKT and Ras/MAPK pathways were identified.

2. Materials and method

2.1. Reagents and materials

ATG, SPA, CLA, CGA, arctiin, deoxycholic acid, glycocholic acid and deoxyglycocholic acid were obtained from Yifang S&T (Tianjin, China). Enzyme-linked immunosorbent assay (ELISA) assay kits of rat TNF-α, IL-6, IL-1β and RANTES, as well as human intracellular proteins (total p38, JNK and ERK), were obtained from Pierce/Endogen Co. (Rockford, Illinois, USA). Human TNF-α was purchased from PeproTech (Rocky Hill, NJ, USA). Dexamethasone (Dex) and levofloxacin (LEV) were purchased from Sigma Chemical Co. (St. Louis, MO, USA). Reagents for cell culture were obtained from Gibco BRL Life Technologies (Rockville, MD, USA). The NF-κB luciferase reporter plasmid pGL4.32 and *Renilla* luciferase reporter vector plasmid pRL-TK were obtained from Promega Co. (Fitchburg, WI, USA). The Lipofectamine 2000 transfection reagent was obtained from Invitrogen (Carlsbad, CA, USA). The anti-IκB-α antibody was obtained from Santa Cruz Biotechnology (San Diego, CA, USA). The *P. aeruginosa* PAK strain, a clinical isolate from the sputum of a patient suffering from bronchiectasis, was provided by Professor Mingqiang Qiao (College of Life Science, Nankai University, China). All other reagents used in this study were of analytical grade.

2.2. Preparation of QF and drugs

Commercial QF (batch No. 5230139) was donated by Tianjin Zhongxin Pharmaceutical Group Co. Ltd., Darentang Pharmaceutical Factory (Tianjin, China). The QF pills were powdered and suspended in distilled water. The QF suspension and LEV were directly diluted with physiological saline for administration to mice. The QF suspension, Dex, ATG, CLA, CGA and SPA were dissolved in dimethylsulfoxide (DMSO) for *in vitro* experiments, and the final concentration of DMSO added to the cells was less than 0.1%.

2.3. Animals and drug administration

Kunming mice (male, 18–22 g) were purchased from the Experimental Animal Center of the National Institute for the Control of Pharmaceutical and Biological Products (Beijing, China). Animal treatment and maintenance were performed in accordance with the Principle of Laboratory Animal Care (NIH Publication No. 85–23, revised 1985), and the Animal Ethics Committee of Nankai University approved the experimental protocol. All animals were housed in separate cages with food and water freely available under standard laboratory conditions of 23–26 °C with a 12 h light/12 h dark cycle. Sixty mice were randomly allotted into six groups, including an uninfected control group (Con) and five *P. aeruginosa* infected groups as follows: model group (Mod), positive control group (LEV) and low/medium/high dose QF groups (QF-L/QF-M/QF-H). LEV (7.5 mg/kg/d) and three doses

of QF (2, 6 or 18 g/kg/d) were administered orally to the mice for one week before *P. aeruginosa* challenge.

2.4. *P. aeruginosa–induced acute lung inflammation*

The acute lung inflammation challenge was performed as previously described[10]. The *P. aeruginosa* PAK strain was used in the experiments and was grown in Luria-Bertani (LB) medium. When necessary, the PAK strain was cultured in duplicate in LB medium overnight, washed twice with phosphate-buffered saline (PBS), resuspended and diluted to a final concentration of 1×10^9 colony-forming units/mL. One week after drug administration, all mice except the control group were challenged with 40 μL of intratracheal PAK suspension (approximately 4×10^7 colony-forming units/lung), after anesthetizing (50 mg/kg sodium pentobarbital, i.p.). The control group was administered the same volume of PBS *via* the same route.

2.5. *Histopathological evaluation*

Twenty-four hours after *P. aeruginosa* challenge, mice were anesthetized by sodium pentobarbital (50 mg/kg, i.p.), and blood samples were collected from the retro-orbital cavity. The serum was separated and the supernatant was collected and stored at −20 °C for subsequent testing. The lungs were collected and placed in 10% formalin for at least 1 week. The organs were embedded in paraffin, sectioned and stained with hematoxylin and eosin (HE). True color photographic images of the slices were taken using a light microscope (Olympus CKX41, Japan).

2.6. *Cell culture, transfection and NF-κB-luciferase assay*

BEAS-2B, a cell line derived from human bronchial epithelial cells, was obtained from the American Type Culture Collection (Rockville, MD, USA) and cultured in RPMI-1640 medium supplemented with 10% fetal bovine serum and 1% penicillin-streptomycin at 37 °C with 5% CO_2 in a humidified incubator. After stimulation by drug and TNF-α, the supernatants were collected for the detection of cytokine and chemokine. Simultaneously, BEAS-2B cells were co-transfected in 96-well plates with the NF-κB luciferase reporter plasmid pGL4.32 and *Renilla* luciferase reporter vector plasmid pRL-TK at 100 and 9.6 ng per well, respectively. Transfection was performed for 24 h using Lipofectamine 2000 according to the manufacturer's instructions. The cells were pretreated with drugs before stimulation by human TNF-α (10 ng/mL) for 6 h. After stimulation, the cells were washed, lysed and assayed for luciferase activity using the Promegadual-luciferase reporter assay system according to the manufacturer's instructions as previously reported[9].

2.7. *Chemokine, cytokine and intracellular proteins measurements*

Cytokines (TNF-α and IL-6), chemokines (IL-8 and RANTES) and intracellular proteins (total p38, JNK and ERK) in the supernatants of plasma, homogenized lungs, cells or cell lysates were measured using commercial ELISA kits according to the manufacturer's instructions. The absorbance of each sample was measured at 450 nm using a Bio-Rad Model 680 microplate reader. Cytokine, chemokine and intracellular protein levels were determined from standard curves and are expressed in picograms per milliliter.

2.8. *Western blot analysis*

BEAS-2B cells were washed with ice-cold PBS and lysed using lysis buffer (2% SDS, 10% glycerol, 62.5 mmol/L Tris–HCl buffer, pH 6.8) for 10 min. A total of 30 μg protein from the cell lysates was transferred to nitrocellulose membranes following separation on 10% SDS-PAGE. The membranes were blocked in 5% skim milk solution overnight, incubated with polyclonal anti-IκB-α antibody (1:500) at 4 °C for 4 h and then washed twice with Tween 20/Tris-buffered saline (TTBS). The blots were subsequently incubated with a secondary horseradish peroxidase-conjugated rabbit antibody for 1 h at room temperature and then washed extensively with TTBS. Detection was performed using an enhanced chemiluminescence kit (Amersham Biosciences, Uppsala, Sweden) as described by the manufacturer, followed by auto-radiography.

2.9. *UPLC/Q-TOF-MS analysis*

The quantitative analysis of anti-inflammatory compounds was performed as previously described with slight modifications[9]. A Waters Acquity UPLC System (Waters Co., Milford, MA) equipped with a photodiode array detector and a Waters Q-TOF Premier with an electrospray ionization (ESI) system (Waters MS Technologies, Manchester, UK) was used. The system was controlled using the MassLynx V4.1 software (Waters Co.). An Acquity BEH C18 column (100 mm × 2.1 mm, 1.7 μm, Waters Co.) was used for the separation. The products were eluted on a gradient of 0.1% *v/v* aqueous formic acid (mobile phase A) and acetonitrile (mobile phase B). The mobile phase gradient was as follows: 5% to 15% B from 0 to 3 min, 15% to 30% B from 3 to 13 min, 30% to 35% B from 13 to 15 min, 35% to 80% B from 15 to 20 min, 80% to 100% B from 20 to 22 min, and 100% to 5% B from 22 to 24 min. The flow was maintained at 5% B from 24 to 30 min. The flow rate was set at 0.4 mL/min, and the column temperature was 30 °C. The experimental conditions for the Q-TOF-MS were the same as previously reported.

2.10. *Quantitative real-time PCR*

After stimulation by drugs (ATG, CLA, CGA or SPA) and TNF-α, the total RNA was extracted from the BEAS-2B cells with TRIzol (Invitrogen, CA, USA) according to the manufacturer's instructions. The cDNA was synthesized using a High-Capacity cDNA Reverse Transcription Kit (Applied Biosystems, CA, USA). PCR amplification was performed and analyzed in triplicate using the GoTaqqPCR Master Mix (Promega), and the emission intensity from the BRYT Green was detected with an iCycler detection system (Bio-Rad, Hercules, CA, USA). The expression levels of each gene were normalized with the internal reference gene, β-actin. The PCR primers for the Ras/MAPK (*p38*, *Jnk*, *Erk*, *Ras* and *Pkc*) and PI3K/AKT pathway (*Pi3k*, *Fak* and *Jak2*) were designed and shown in Table 1.

2.11. *Target prediction and molecular docking*

Anti-inflammatory candidate compounds were selected and their structures were saved in mol2 format file, and placed into the PharmMapper database (http://59.78.96.61/pharmmapper/) for tar get prediction. Annotation and pathway analysis were performed using the Kyoto Encyclopedia of Genes and Genomes (KEGG) (http://www.genome.jp/kegg/). To further evaluate the selectivity of targets, a series of candidate molecules were optimized using

Table 1 Primers and probes for real-time RT-PCR.

Gene	Primers sequence
p38	Forward-5′-TCCAGACCATTTCAGTCCATC-3′
	Reverse-5′-CGTCCAACAGACCAATCACAT-3′
Erk	Forward-5′-GCCCGAAACTACCTACAGTCTC-3′
	Reverse-5′-CCGTTTATTGGGGTT-AAAGGTT-3′
Jnk	Forward-5′-TGGGTATGGGCTACAAAGAGA-3′
	Reverse-5′-TTCCTCACAGTTGGCTGAAGT-3′
Fak	Forward-5′-ATCCCACACATCTTGCTGACTT-3′
	Reverse-5′-GCATTCCTTTTCTGTCCTTGTC-3′
Jak2	Forward-5′-AAGCAGCAAGTATGATGAGCAA-3′
	Reverse-5′-TCCCATGAATAAGGGTGTTTTC-3′
Pi3k	Forward-5′-CCTGCTTTTGGAGTCCTATTGT-3′
	Reverse-5′-ATCTGGTCGCCTCATTTGC-3′
Ras	Forward-5′-GGGTGAAGGACTCGGATGAC-3′
	Reverse-5′-ATGTAGGGGATGCCGTAGCT-3′
Pkc	Forward-5′-TATGGAAAATCTGTGGACTGGTG-3′
	Reverse-5′-CTTGGCTGGGTGTTTGGTC-3′
β-actin	Forward-5′-GACAGGATGCAGAAGGAGAT-3′
	Reverse-5′-TGCTTGCTGATCCACATCTG-3′

SYBYL X2.0 and then docked to the targets. The crystal structures of the potential target proteins were obtained from the Protein Data Bank (ID: 2R7B, 3V6R, 3WJ6, 3EQF, 4J8F, 4EFL and 4EKK, http://www.rcsb.org/pdb). At this stage, the target structures were preprocessed and prepared by deleting all water molecules and hydrogen atoms were then added. Next, a grid box was generated before docking. The PDBQT files of targets and ligands were prepared using AutoDockTools. The center of the grids was placed on the center of the mass of ligands. A genetic algorithm (GA) was used to simulate ligand-receptor binding. The number of GA runs was 30. The step size parameters of quaternion and torsion were set to 30. For each compound, 30 independent runs were performed. Default values were used for all other parameters.

2.12. Statistical analysis

The data are expressed as the mean ± standard deviation (SD) of at least 3 independent experiments. One-way ANOVA and student's *t*-test were used for statistical analysis. Differences were considered statistically significant if the P value was less than 0.05.

3. Results

3.1. Effects of QF on pulmonary histopathology and the production of cytokines

To evaluate the effects of QF on acute lung inflammation, the cross-sections of lung tissue of HE staining are shown in Fig. 1A. PAK strain infection caused capillary congestion, obstruction of small airways by lymphocytic infiltrates, and widened alveolar septa compared to the structural integrity of the lung tissue in the control group. Pretreatment with medium and high-dose QF significantly reduced histological injury, with less obstruction of small airways and recruitment of inflammatory infiltrates ($P<0.05$ and $P<0.01$, respectively). However, histological damage was not improved by low-dose QF. The evidence indicated that medium and high-dose QF ameliorated *P. aeruginosa*–induced lung infection in mice.

TNF-α, a pro-inflammatory factor, activates the expression of many other cytokines and chemotactic factors and induces severe pulmonary tissue injury[11]. IL-6 is a representative cytokine that stimulates mucous secretion and promotes the differentiation of B cells and the cytotoxicity of T cells and mast cells[12]. IL-8 can induce immune cell infiltration, and RANTES causes mononuclear leukocytes and eosinophilic granulocytes to participate in inflammation[13,14]. After *P. aeruginosa* challenge, levels of cytokines and chemokines in the plasma and lung homogenate were measured by ELISA. TNF-α, IL-6, IL-8 and RANTES were significantly increased in both the plasma and lung tissue after *P. aeruginosa* infection. As shown in Fig. 1, pretreatment with low dose QF did not prevent the release of TNF-α, IL-6, and RANTES; however, treatment at medium and high dose QF decreased the production of these cytokines in different degrees ($P<0.05$ and $P<0.001$, respectively). Only high dose QF decreased the release of RANTES ($P<0.05$). These results were consistent with the histological changes noted above.

3.2. Effects of QF on cytokine activation and IκB-α degradation in bronchial epithelial cells

The effects of QF on the production of cytokines were also studied on bronchial epithelial cells *in vitro*. Pretreatment for 4 h with different doses of QF (QF-L, 0.1 mg/mL; QF-M, 0.5 mg/mL; QF-H, 2.5 mg/mL) was performed, followed by 10 ng/mL TNF-α stimulation for 6 h. The positive control, Dex (1 μmol/L), and the medium and high-dose QF significantly suppressed IL-6 and IL-8 expression (Fig. 2A, B) and NF-κB activation compared to the model group ($P<0.05$ and $P<0.01$, Fig. 2C). However, the low dose QF had no inhibitory effect. To verify the effect of QF-mediated inhibition of NF-κB, western blotting was used to determine whether QF inhibited TNF-α stimulated IκB-α degradation. As shown in Fig. 2D, IκB-α degradation induced by TNF-α is suppressed by QF in a dose-dependent manner. These results demonstrate the anti-inflammatory effects of QF at the cellular level.

3.3. Quantitative analysis of anti-inflammatory ingredients

To clarify the content of the anti-inflammatory ingredients, UPLC/Q-TOF-MS was used to identify the amount of arctiin (ATG-4-glucoside), SPA, CGA and CLA derivatives in QF (Fig. 3). Compared to CGA (2.18 μg/mL) and SPA (0.35 μg/mL), the amount of ATG-4-glucoside (29.94 μg/mL) and total CLA derivatives (50.65 μg/mL), including CLA (22.09 μg/mL), deoxycholic acid (11.95 μg/mL), glycocholic acid (11.94 μg/mL) and deoxyglycocholic acid (4.67 μg/mL), are higher in QF. ATG is the primary metabolite after oral administration of arctiin[15]. Therefore, ATG and CLA were predicted to play a major role in the anti-inflammatory process. These compounds were derived from the Fructus Arctii and Bovis Calculus, respectively.

3.4. Effects of four anti-inflammatory ingredients on candidate gene expression

To investigate the possible anti-inflammatory mechanism, the expression of critical genes of the PI3K/AKT and Ras/MAPK pathways that was proved to be effective for QF-H group (data not shown) was determined using quantitative RT-PCR. As shown in Fig. 4, the mRNA expression of *p38*, *Jnk*, *Erk*, *Fak*, *Pi3k*, *Ras*, *Jak2* and *Pkc* were up-regulated greatly after TNF-α (10 ng/mL) stimulation for 6 h in the model group. Compared to the model

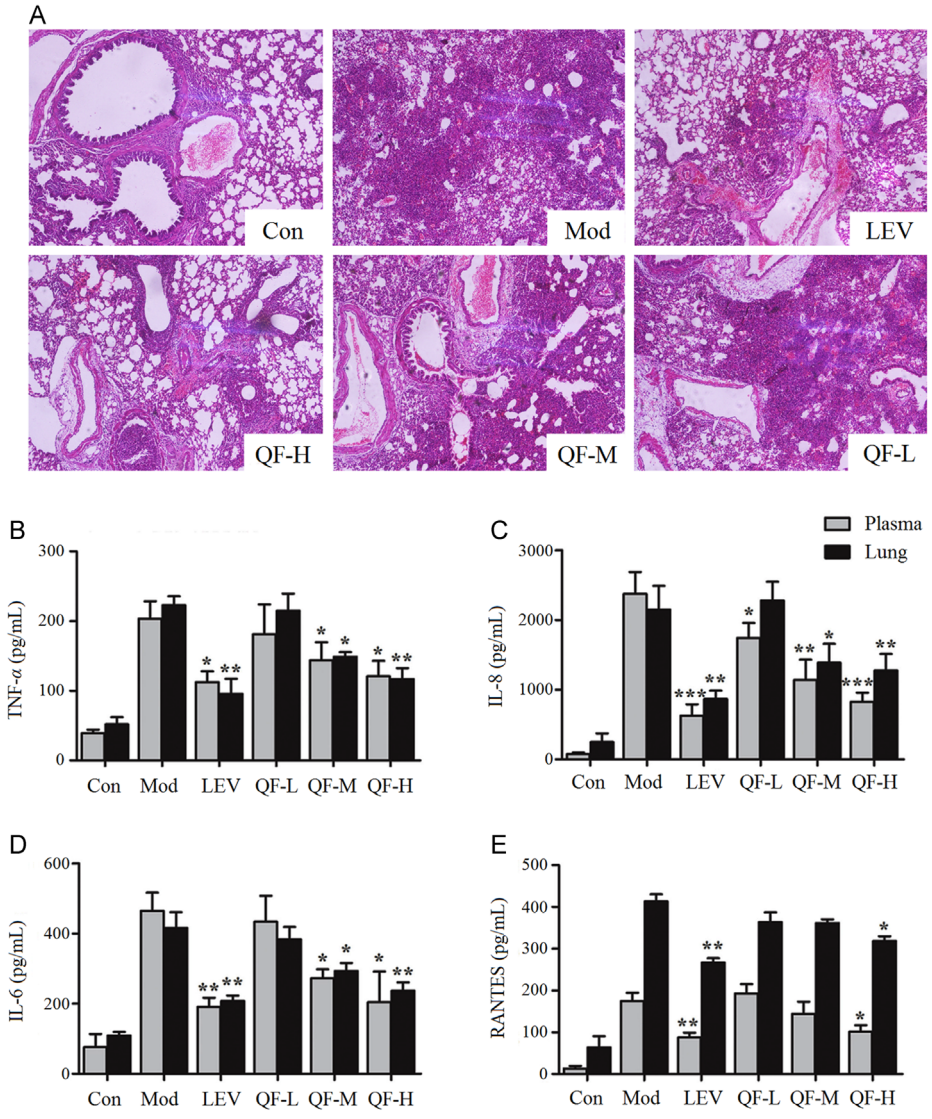

Figure 1 Effects of QF administration on acute lung inflammation induced by *P. aeruginosa*. (A) HE staining of lung sections. The pictures were taken under light microscopy at 100 × magnification; effects of QF on the production of (B) TNF-α, (C) IL-8, (D) IL-6 and (E) RANTES in the plasma and homogenized lung. The values are presented as mean ± SD; $^{*}P<0.05$, $^{**}P<0.01$ and $^{***}P<0.001$ *vs*. model group ($n=5$).

group, pretreatment for 2 h with ATG inhibited the expression of all genes significantly ($P<0.05$). However, the other compounds had different inhibitory effects. The Ras/MAPK-related gene expression of *p38*, *Erk* ($P<0.05$) and *Ras* ($P<0.01$) was significantly decreased with CLA pretreatment. CGA suppressed the expression of *p38*, *Jnk* ($P<0.05$) and *Pi3k* ($P<0.01$). Furthermore, SPA inhibited the expression of *p38*, *Jnk*, *Erk*, *Ras* ($P<0.05$) and *Pi3k, Fak* ($P<0.05$). These results indicated that CLA only affected the Ras/MAPK pathway, but ATG, CGA and SPA affected both the PI3K/AKT and Ras/MAPK pathways.

3.5. *Synergistic effects of anti-inflammatory ingredients on PI3K/AKT pathway*

PI3K/AKT and Ras/MAPK pathways have similar functions and have complex interactions[16] p38 kinase-dependent MAPK has an activating function for AKT[17] and PI3K/AKT is activated by low-molecular-weight GTP/GDP binding GTPases, such as Ras, to further regulate the expression of NF-κB[18]. To elucidate the synergistic effect on PI3K/AKT/NF-κB, the combination treatment of the above four ingredients was detected by downstream NF-κB-dependent signal transduction (Fig. 5). Treatment with ATG, CLA, CGA or SPA decreased NF-κB dependent transcription ($P<0.05$). When ATG was combined with CLA, CGA and SPA, or all together, the inhibition was greater than for any one drug ($P<0.01$ and $P<0.001$). These results indicate that ATG is the most important inhibitor of the PI3K/AKT pathway.

3.6. *Intracellular MAPK proteins levels validation of p38, JNK, and ERK*

MAPK has three family members, p38, JNK and ERK. PI3K inhibitors decrease the activity of the Ras/MAPK pathway[19]. The effects of single or combination treatment with different inhibitors on p38, JNK and ERK intracellular proteins levels in TNF-α (10 ng/mL) stimulated BEAS-2B cells were validated by ELISA. As shown in Fig. 6, treatment with ATG alone significantly suppressed the levels of p38,

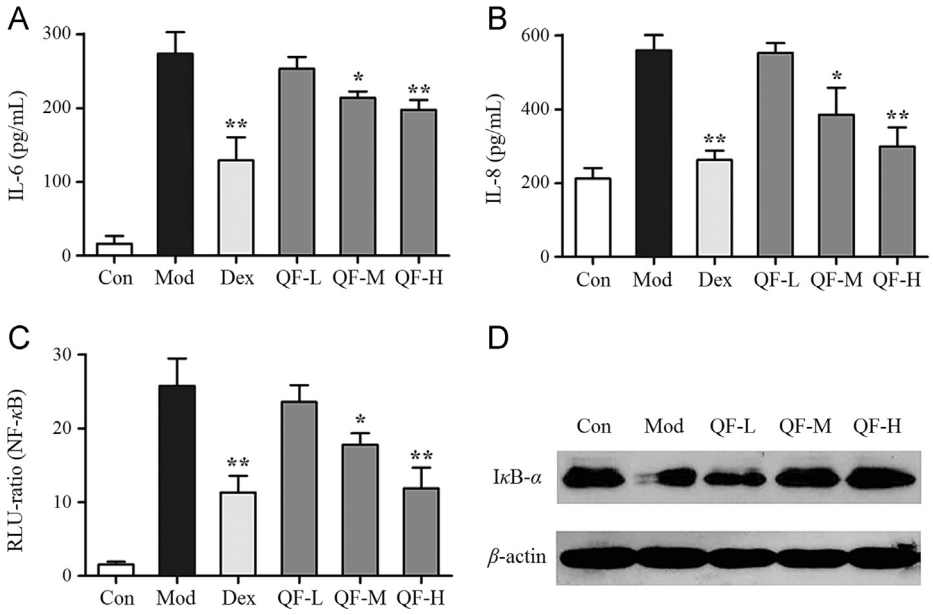

Figure 2 Effects of QF in TNF-α stimulated BEAS-2B cells. (A) IL-6 expression and (B) IL-8 expression determined by ELISA; (C) NF-κB activation detected by luciferase activity analysis; (D) IκB-α protein degradation analyzed by western blot. The values shown are mean $\pm$ SD of 5 independent experiments; $^{*}P<0.05$ and $^{**}P<0.01$ *vs*. model group ($n=5$).

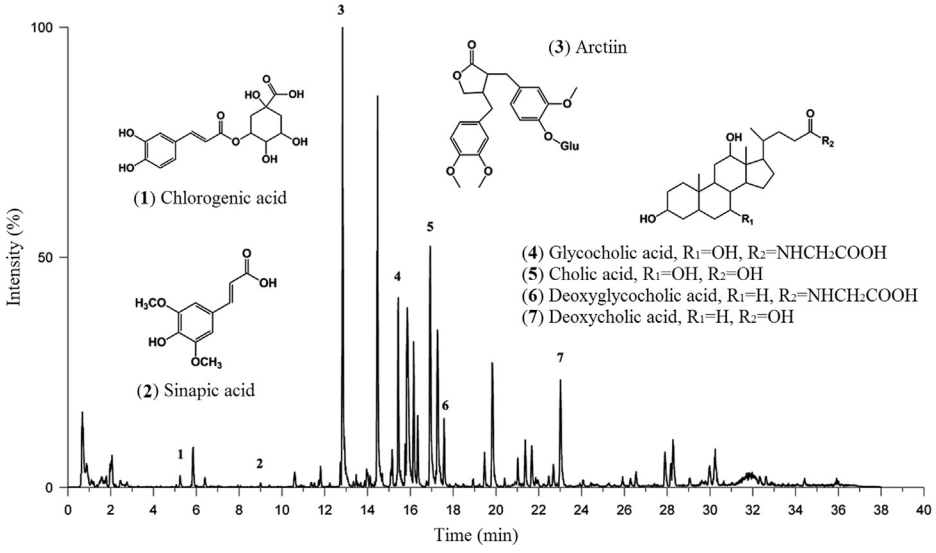

Figure 3 Base peak intensity chromatogram in negative ion modes for QF.

JNK, and ERK ($P<0.01$). CGA suppressed the expression of p38 and JNK ($P<0.05$). CLA reduced p38 and ERK ($P<0.05$) and SPA only down-regulated the p38 level ($P<0.01$). For paired applications, the synergistic effect of ATG combined with CLA suppressed the p38 and ERK levels ($P<0.001$), whereas ATG combined with CGA or SPA primarily affected the p38 and JNK levels ($P<0.001$).

3.7. Target docking of active ingredients and anti-inflammatory network analysis

To explore potential protein targets, a pharmacophore matching platform, PharmMapper server, was utilized for target docking in the PI3K/AKT and Ras/MAPK pathways. Molecular docking validation was performed with AutoDock 4.0, providing further detailed information for the representational ligands and regulated targets, including ATG for PDK1 (-7.24 kcal/mol) and JNK (-8.99 kcal/mol), CLA for FGFR (-8.16 kcal/mol) and MEK (-9.86 kcal/mol), and CGA for Ras (-7.16 kcal/mol), HSPA (-8.06 kcal/mol) and Rac (-6.24 kcal/mol), which showed higher scores for the PI3K/AKT and Ras/MAPK pathways identifying them as potential targets. However, SPA for PDK1 (-5.10 kcal/mol), FGFR (-5.38 kcal/mol), Ras (-4.39 kcal/mol) and Rac (-5.21 kcal/mol) had a lower binding energy and were omitted from further analysis. The detail interaction information of the key targets and related compound is shown in Fig. 7.

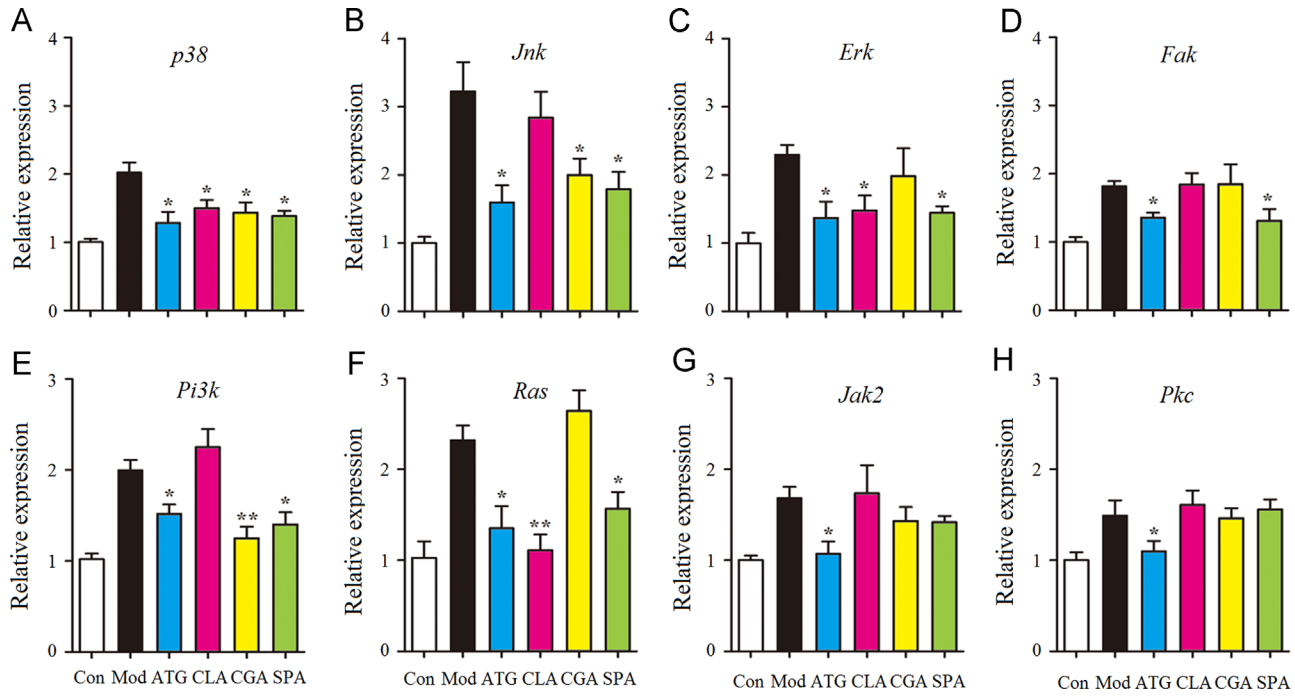

Figure 4 Effects of anti-inflammatory compounds from QF on gene expression in TNF-α stimulated BEAS-2B cells. The mRNA expression of *p38* (A), *Jnk* (B), *Erk* (C), *Fak* (D), *Pi3k* (E), *Ras* (F), *Jak2* (G) and *Pkc* (H) was quantified by real-time PCR. Relative expression levels of the genes were normalized to β-actin as an internal reference. The results are expressed as mean $\pm$ SD from 3 independent experiments; $^{*}P<0.05$ and $^{**}P<0.01$ *vs*. model group ($n=3$).

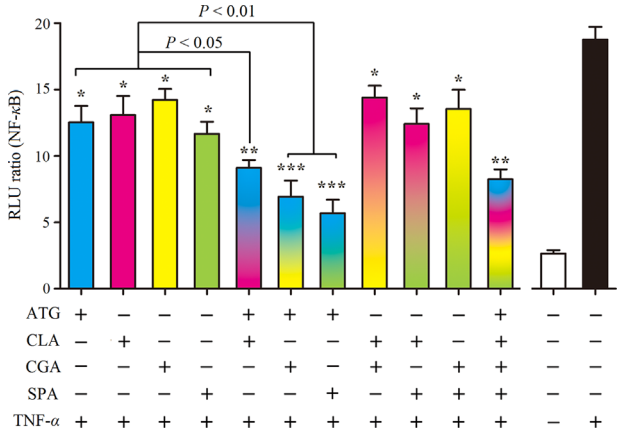

Figure 5 Effects of anti-inflammatory compounds from QF on NF-κB activation in TNF-α stimulated BEAS-2B cells. ATG, CLA, CGA and SPA were administered at 50 μmol/L when used alone, 25 μmol/L for paired combinations, and 12.5 μmol/L for combinations of 4 drugs. The values shown are mean$\pm$SD of 4 independent experiments; $^{*}P<0.05$, $^{**}P<0.01$ and $^{***}P<0.001$ *vs*. group treated with TNF-α in the absence of drugs ($n=6$).

Based on the KEGG analysis and the above result, the key anti-inflammatory network for QF and the PI3K/AKT and Ras/MAPK pathways is summarized in Fig. 7.

4. Discussion

P. aeruginosa–induced pneumonia is a complex process. First, large numbers of thalli aggregating in the air way utilize flagellum, fimbriae, and polysaccharides on the membrane surface to adhere to respiratory epithelia[20,21]. Then, the immune response of the host is activated *via* invasion of the type III secretory protein, quorum-sensing system, pyocyanin, LPS and other virulence factors. Consequently, cytokines, chemotactic factors and other inflammatory mediators are produced by host cells, which recruit and activate macrophages, neutrophilic granulocytes, and T cells, resulting in severe lung injury and mortality[22–24]. In this study, we established a mouse acute pneumonia model with *P. aeruginosa* and the protective effects of QF were estimated by evaluating the expression of inflammatory mediators and the histopathological condition. The results indicate that pretreatment with QF significantly inhibits the release of cytokines (TNF-α, IL-6) and chemokines (IL-8, RANTES), reduces leukocytes recruitment into inflamed tissues, ameliorates pulmonary edema and necrosis, and promotes the survival of mice.

PI3K/AKT and Ras/MAPK are two important pathways for cell membrane receptor signal transduction, which are involved in both the inflammatory and immune response[25, 26]. LPS activates PKC and initiates pro-inflammatory signals, such as FAK and Ras[27]. FAK, a protein tyrosine kinase, can activate PI3K and MAPK to regulate the expression of cytokines in the immune and inflammatory responses[28,29]. Furthermore, Ras is a GTPase, which activates ERK and p38 to regulate the generation of inflammatory factors[30]. By contrast, after binding to membrane receptors or activating JAK, cytokines and other growth factor can activate PI3K and MAPKs to regulate the proliferation and differentiation of cells and the expression of pro-inflammatory factors[31]. The pro-inflammatory factor TNF-α is not only a basic factor of the inflammatory response, but it also acts on Gram-negative bacteria through a positive feedback pathway and synergistically enhances the infection[32]. In this study, cultured BEAS-2B cells induced with TNF-α were selected for the inflammation model to assess the anti-

inflammatory effect of QF *in vitro*. Four candidate compounds from QF were then selected to determine the synergistic anti-inflammatory mechanisms.

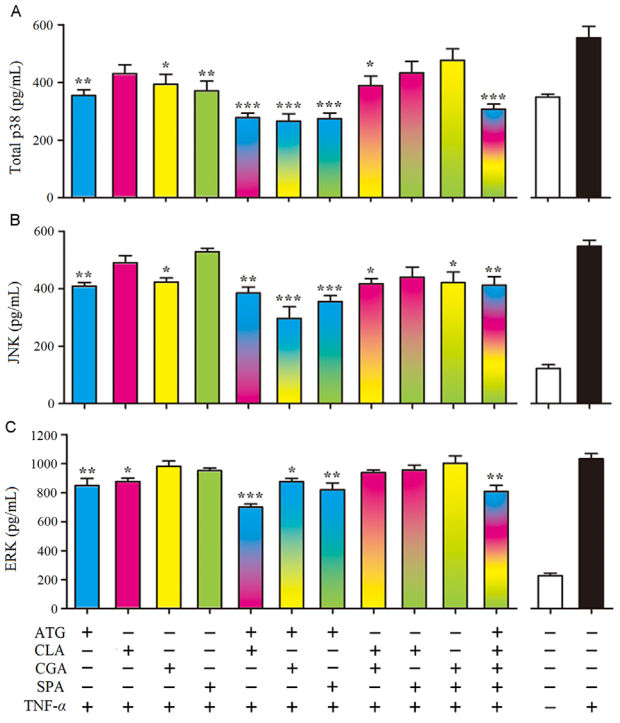

Figure 6 Effects of anti-inflammatory compounds from QF on the intracellular protein expressions of (A) p38, (B) JNK, and (C) ERK in BEAS-2B cells. ATG, CLA, CGA, and SPA were administered at 50 μmol/L when used alone, 25 μmol/L for paired combinations, and 12.5 μmol/L for combinations of 4 drugs. The cells were lysed after drug and TNF-α stimulation, and the cell lysates were analyzed by ELISA for p38, JNK, and ERK levels. The values shown are mean ±SD of 6 independent experiments; $^{*}P<0.05$, $^{**}P<0.01$ and $^{***}P<0.001$ *vs.* group treated with TNF-α in the absence of drugs ($n=6$).

ATG is a representative dibenzyl butyrolactone lignan with anti-inflammatory, anti-viral, anti-tumor, and Ca^{2+} antagonist activities[33]. Its anti-inflammatory mechanisms include suppression of the overproduction of NO by inhibiting the JAK-STAT signal pathway in LPS-stimulated macrophages[34,35] inhibition of AKT phosphorylation and amelioration of inflammation by inhibiting the PI3K/AKT pathway[36,37] regulation of the activation of MAP kinases, leading to AP-1 inactivation and the production of TNF-α[38]. In this study, ATG was predicted target to PDK1 and downregulate the phosphorylation of AKT and PKC, and further affect the expression of the downstream genes, NF-κB and MAP kinases.

CGA significantly inhibits the expression of COX-2 and iNOS, attenuates inflammation-related markers, such as IL-1β, TNF-α, IL-6, and ninjurin1 (Ninj1), abolishes the phosphorylation of Akt, p38, ERK, and down regulates a receptor activator of the NF-κB ligand induced nuclear factor of activated T cells c1 (NFATc1) expression[39,40]. Additionally, the effects of CGA against LPS-induced inflammation may be due to its ability to attenuate the TLR4-mediated NF-κB signaling pathway[41]. In this study CGA has been suggested to bind to the Ras protein, and when combined with ATG affects the p38 and ERK pathways. These results were consistent with previous reports.

In addition, the mechanism of the anti-inflammatory effects of CLA and SPA for the suppression of TNF-α and IL-1β expression *via* NF-κB was shown in previous studies[42,43]. In this study, CLA simultaneously targeted the upstream protein FGFR and the downstream protein MEK of the Ras/MAPK pathway, which was speculated firstly. When combined with ATG, the effect also occurred on the p38 and ERK sub-pathway. SPA has a smaller molecular structure and the binding activities were also weaker. Furthermore, because of its low content, SPA did not play a major role in the overall anti-inflammatory effect.

In summary, a network mechanism of several ingredients was identified from QF and mutual suppression was demonstrated on the regulation of primary intracellular immune response to ameliorate acute pneumonia induced by *P. aeruginosa*. ATG was the principal ingredient responsible for the anti-inflammatory effect both on the PI3K/AKT and Ras/MAPK pathways. The other ingredients, CLA, and CGA, enhanced the

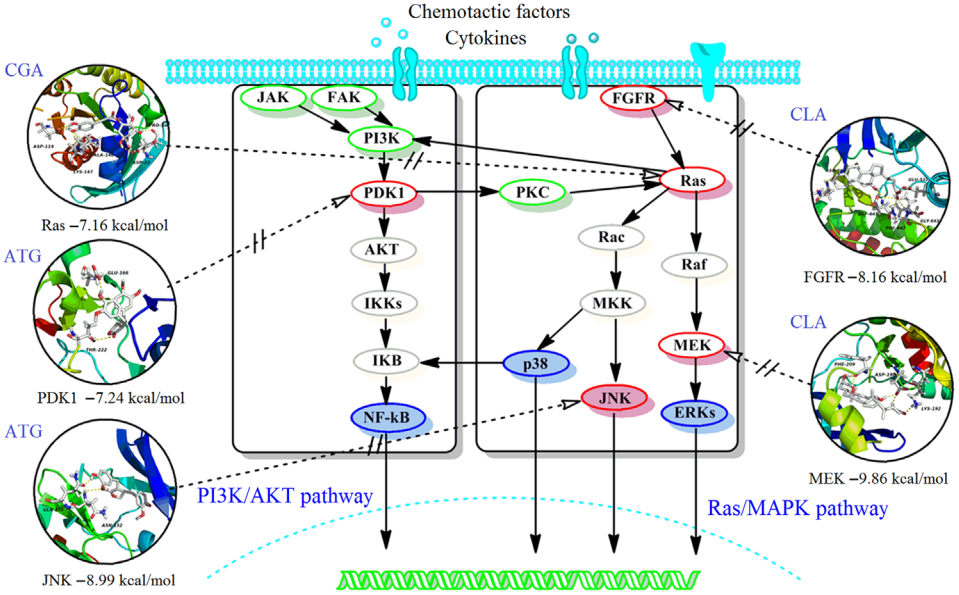

Figure 7 The scheme of the proposed network anti-inflammatory mechanisms for QF in the PI3K/AKT and Ras/MAPK pathways.

actions of ATG and showed synergistic NF-κB inactivation effects, possibly *via* the Ras/MAPK signal pathway.

Acknowledgments

This work was supported by the National Natural Science Foundation of China (Nos. 81173638 and 81373506) and the Key Program of Natural Science of Foundation of Tianjin, China (No.13JCZDJC31400).

References

1. Normile D. The new face of traditional Chinese medicine. *Science* 2003;**299**:188–90.
2. Liu CX, Liu R, Fan HR, Xiao XF, Chen XP, Xu HY, et al. Network pharmacology bridges traditional application and modern development of traditional Chinese medicine. *Chin Herb Med* 2015;**7**:3–17.
3. Li S. Mapping ancient remedies: applying a network approach to traditional Chinese medicine. *Science* 2015;**350**:S72–4.
4. Xutian S, Cao DY, Wozniak J, Junion J, Boisvert J. Comprehension of the unique characteristics of traditional Chinese medicine. *Am J Chin Med* 2012;**40**:231–44.
5. Chen Y, Guo JJ, Healy DP, Zhan S. Effect of integrated traditional Chinese medicine and Western medicine on the treatment of severe acute respiratory syndrome: a meta-analysis. *Pharm Pract* 2007;**5**:1–9.
6. Liu Q, Lu L, Hua ML, Xu Y, Xiong HR, Hou W, et al. Jiawei-Yupingfeng-Tang, a Chinese herbal formula, inhibits respiratory viral infections *in vitro* and *in vivo*. *J Ethnopharmacol* 2013;**150**:521–8.
7. Hou YY, Cheng BF, Zhou MG, Fang RP, Jiang M, Hou WB, et al. Searching for synergistic bronchodilators and novel therapeutic regimens for chronic lung diseases from a traditional Chinese medicine, Qingfei Xiaoyan Wan. *PLoS One* 2014;**9**:e113104.
8. Zhao ZY, Miao YB, Pan PW, Cheng BF, Bai G, Wu H. Qingfei Xiaoyan Wan alleviates asthma through multi-target network regulation. *BMC Complement Altern Med* 2013;**13**:206.
9. Cheng BF, Hou YY, Wang LQ, Dong LY, Peng JM, Bai G. Dual-bioactivity-based liquid chromatography-coupled quadrupole time-of-flight mass spectrometry for NF-κB inhibitors and β2AR agonists identification in Chinese medicinal preparation Qingfei XiaoyanWan. *Anal Bioanal Chem* 2012;**404**:2445–52.
10. Bai F, Xu HJ, Zhang Q, Qi XZ, Mou R, Bai G, et al. Functional characterization of *pfm* in protein secretion and lung infection of *Pseudomonas aeruginosa*. *Can J Microbiol* 2011;**57**:829–37.
11. Thacker EL. Lung inflammatory responses. *Vet Res* 2006;**37**:469–86.
12. Gerthoffer WT, Singer CA. MAPK regulation of gene expression in airway smooth muscle. *Respir Physiol Neurobiol* 2003;**137**:237–50.
13. Chmura K, Bai X, Nakamura M, Kandasamy P, McGibney M, Kuronuma K, et al. Induction of IL-8 by *Mycoplasma pneumoniae* membrane in BEAS-2B cells. *Am J Physiol Lung Cell Mol Physiol* 2008;**295**:L220–30.
14. Lampinen M, Carlson M, Håkansson LD, Venge P. Cytokine-regulated accumulation of eosinophils in inflammatory disease. *Allergy* 2004;**59**:793–805.
15. He F, Dou DQ, Sun Y, Zhu L, Xiao HB, Kang TG. Plasma pharmacokinetics and tissue distribution of arctiin and its main metabolite in rats by HPLC–UV and LC–MS. *Planta Med* 2012;**78**:800–6.
16. Lee Jr. JT, McCubrey JA. The Raf/MEK/ERK signal transduction cascade as a target for chemotherapeutic intervention in leukemia. *Leukemia* 2002;**16**:486–507.
17. Rane MJ, Coxon PY, Powell DW, Webster R, Klein JB, Pierce W, et al. P38 kinase-dependent MAPKAPK-2 activation functions as 3-phosphoiinositide-dependent kinase-2 for AKT in human neutrophils. *J Biol Chem* 2001;**276**:3517–23.
18. Lin HH, Chen JH, Chou FP, Wang CJ. Protocatechuic acid inhibits cancer cell metastasis involving the down-regulation of Ras/Akt/NF-κB pathway and MMP-2 production by targeting RhoB activation. *Br J Pharmacol* 2011;**162**:237–54.
19. Steelman LS, Pohnert SC, Shelton JG, Franklin RA, Bertrand FE, McCubrey JA. JAK/STAT, Raf/MEK/ERK, PI3K/AKT and BCR-ABL in cell cycle progression and leukemogenesis. *Leukemia* 2004;**18**:189–218.
20. Stover CK, Pham XQ, Erwin AL, Mizoguchi SD, Warrener P, Hickey MJ, et al. Complete genome sequence of *Pseudomonas aeruginosa* PAO1, an opportunistic pathogen. *Nature* 2000;**406**:959–64.
21. Gellatly SL, Hancock RE. *Pseudomonas aeruginosa*: new insights into pathogenesis and host defenses. *Pathog Dis* 2013;**67**:159–73.
22. Driscoll JA, Brody SL, Kollef MH. The epidemiology, pathogenesis and treatment of *Pseudomonas aeruginosa* infections. *Drugs* 2007;**67**:351–68.
23. Hauser AR, Cobb E, Bodi M, Mariscal D, Vallés J, Engel JN, et al. Type III protein secretion is associated with poor clinical outcomes in patients with ventilator-associated pneumonia caused by *Pseudomonas aeruginosa*. *Crit Care Med* 2002;**30**:521–8.
24. Sadikot RT, Blackwell TS, Christman JW, Prince AS. Pathogen-host interactions in *Pseudomonas aeruginosa* pneumonia. *Am J Respir Crit Care Med* 2005;**171**:1209–23.
25. Kyriakis JM, Avruch J. Mammalian mitogen-activated protein kinase signal transduction pathways activated by stress and inflammation. *Physiol Rev* 2001;**81**:807–69.
26. Zhang YP, Cardell LO, Edvinsson L, Xu CB. MAPK/NF-κB-dependent upregulation of kinin receptors mediates airway hyperreactivity: a new perspective for the treatment. *Pharmacol Res* 2013;**71**:9–18.
27. Diaz-Meco MT, Moscat J. The atypical PKCs in inflammation: NF-κB and beyond. *Immunol Rev* 2012;**246**:154–67.
28. Schaller MD. Biochemical signals and biological responses elicited by the focal adhesion kinase. *Biochim Biophys Acta* 2001;**1540**:1–21.
29. Schlaepfer DD, Hou SH, Lim ST, Tomar A, Yu HG, Lim Y, et al. Tumor necrosis factor-α stimulates focal adhesion kinase activity required for mitogen-activated kinase-associated interleukin 6 expression. *J Biol Chem* 2007;**282**:17450–9.
30. Johnson DS, Chen YH. Ras family of small GTPases in immunity and inflammation. *Curr Opin Pharmacol* 2012;**12**:458–63.
31. Tripathi A, Sodhi A. Growth hormone–induced production of cytokines in murine peritoneal macrophages *in vitro*: role of JAK/STAT, PI3K, PKC and MAP kinases. *Immunobiology* 2009;**214**:430–40.
32. Gosselin D, DeSanctis J, Boulé M, Skamene E, Matouk C, Radzioch D. Role of tumor necrosis factor α in innate resistance to mouse pulmonary infection with *Pseudomonas aeruginosa*. *Infect Immun* 1995;**63**:3272–8.
33. Kang HS, Lee JY, Kim CJ. Anti-inflammatory activity of arctigenin from Forsythiae Fructus. *J Ethnopharmacol* 2008;**116**:305–12.
34. Kou XJ, Qi SM, Dai WX, Luo L, Yin ZM. Arctigenin inhibits lipopolysaccharide-induced iNOS expression in RAW264.7 cells through suppressing JAK–STAT signal pathway. *Int Immunopharmacol* 2011;**11**:1095–102.
35. Zhao F, Wang L, Liu K. *In vitro* anti-inflammatory effects of arctigenin, a lignan from *Arctium lappa* L., through inhibition on iNOS pathway. *J Ethnopharmacol* 2009;**122**:457–62.
36. Awale S, Lu J, Kalauni SK, Kurashima Y, Tezuka Y, Kadota S, et al. Identification of arctigenin as an antitumor agent having the ability to eliminate the tolerance of cancer cells to nutrient starvation. *Cancer Res* 2006;**66**:1751–7.
37. Hyam SR, Lee IA, Gu W, Kim KA, Jeong JJ, Jang SE, et al. Arctigenin ameliorates inflammation *in vitro* and *in vivo* by inhibiting the PI3K/AKT pathway and polarizing M1 macrophagesto M2-like macrophages. *Eur J Pharmacol* 2013;**708**:21–9.
38. Cho MK, Jang YP, Kim YC, Kim SG. Arctigenin, a phenylpropanoid dibenzyl butyrolactone lignan, inhibits MAP kinases and AP-1

activation *via* potent MKK inhibition: the role in TNF-α inhibition. *Int Immunopharmacol* 2004;**4**:1419–29.

39. Kwak SC, Lee C, Kim JY, Oh HM, So HS, Lee MS, et al. Chlorogenic acid inhibits osteoclast differentiation and bone resorption by down-regulation of receptor activator of nuclear factor κB ligand–induced nuclear factor of activated T cells c1 expression. *Biol Pharm Bull* 2013;**36**:1779–86.
40. Hwang SJ, Kim YW, Park Y, Lee HJ, Kim KW. Anti-inflammatory effects of chlorogenic acid in lipopolysaccharide-stimulated RAW 264.7 cells. *Inflamm Res* 2014;**63**:81–90.
41. Gao RF, Fu YH, Wei ZK, Zhou ES, Li YM, Yao MJ, et al. Chlorogenic acid attenuates lipopolysaccharide-induced mice mastitis by suppressing TLR4-mediated NF-κB signaling pathway. *Eur J Pharmacol* 2014;**729**:54–8.
42. Yun KJ, Koh DJ, Kim SH, Park SJ, Ryu JH, Kim DG, et al. Anti-inflammatory effects of sinapic acid through the suppression of inducible nitric oxide synthase, cyclooxygase-2, and proinflammatory cytokines expressions *via* nuclear factor-κB inactivation. *J Agric Food Chem* 2008;**56**:10265–72.
43. Hua Q, Zhu XL, Li PT, Liu Y, Zhang N, Xu Y, et al. The inhibitory effects of cholalic acid and hyodeoxycholalic acid on the expression of TNFα and IL-1β after cerebral ischemia in rats. *Arch Pharm Res* 2009;**32**:65–73.